

BEAMLINE

U7A, X7B, and X19A

PUBLICATION

G. Liu et al, "Adsorption and Reaction of SO_2 on Model $\text{Ce}_{1-x}\text{Zr}_x\text{O}_2(111)$ Catalysts", *J. Phys. Chem. B*, **108**, 2931 (2004).

FUNDING

U.S. Department of Energy
Interministerial Committee on Science and Technology (CICYT, Spain)

FOR MORE INFORMATION

José A. Rodríguez, Chemistry Department, Brookhaven National Laboratory
rodriguez@bnl.gov

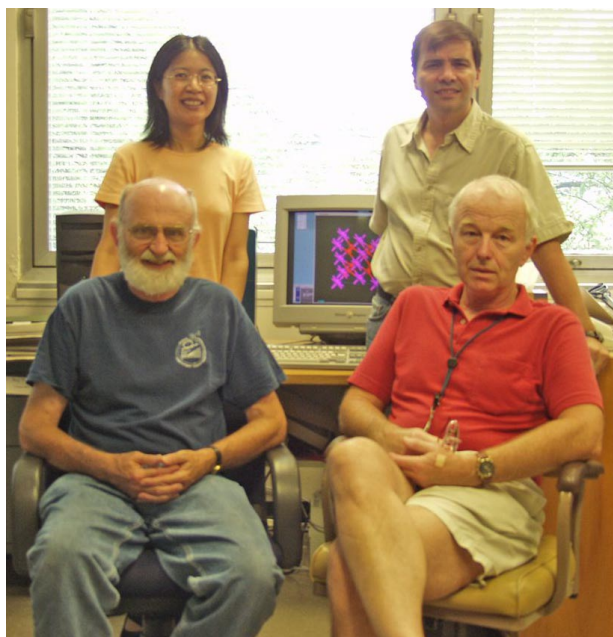
Chemistry of SO_2 on $\text{Ce}_{1-x}\text{Zr}_x\text{O}_2$ Nanoparticles and $\text{Ce}_{1-x}\text{Zr}_x\text{O}_2(111)$ Surfaces

J.A. Rodríguez¹, X. Wang¹, G. Liu¹, J. Hanson¹, J. Hrbek¹, C.H.F. Peden², A. Iglesias-Juez³ and M. Fernández-García³

¹Brookhaven National Laboratory; ²Pacific Northwest National Laboratory, Richland; ³Instituto de Catálisis y Petroleoquímica, Madrid, Spain

A major effort in environmental cleanup is controlling the emission of toxic pollutants produced during the combustion of fuels in factories, power plants, and automotive engines. Cerium oxide (CeO_2)-based materials are utilized as catalysts for the destruction of one of these pollutants, sulfur dioxide (SO_2), and are also used to prevent acid rain. High-resolution photoemission, time-resolved x-ray diffraction (TR-XRD), and x-ray absorption near-edge spectroscopy (XANES) were used to investigate the chemistry of SO_2 on cerium oxide-zirconium ($\text{Ce}_{1-x}\text{Zr}_x\text{O}_2$) nanoparticles and $\text{Ce}_{1-x}\text{Zr}_x\text{O}_2(111)$ surfaces ($x \leq 0.5$). S K-edge XANES spectra pointed to sulfate (SO_4) as the main product of the adsorption of SO_2 on these mixed-metal oxides. Full SO_2 dissociation was seen on the nanoparticles, but not on the $\text{Ce}_{1-x}\text{Zr}_x\text{O}_2(111)$ surfaces. The metal cations at corner or edge sites of the $\text{Ce}_{1-x}\text{Zr}_x\text{O}_2$ nanoparticles probably play a very important role in interactions with the SO_2 molecules.

The $\text{Ce}_{1-x}\text{Zr}_x\text{O}_2$ system is one of the most studied mixed-metal oxides in the literature. Typically, the Ce and Zr cations are randomly distributed in a fluorite-type structure. The focus has been on examining possible correlations between the $\text{CeO}_2:\text{ZrO}_2$ interactions and differences in the behavior of $\text{Ce}_{1-x}\text{Zr}_x\text{O}_2$ and CeO_2 . Oxide nanostructures can have special chemical properties due to size-induced structural distortions and the presence of corner sites and oxygen vacancies. Recent studies have shown that $\text{Ce}_{1-x}\text{Zr}_x\text{O}_2$ nanoparticles can be prepared by a novel microemulsion method that leads to materials with highly homogenous chemical compositions (i.e. Ce,Zr distribution) and a narrow distribution of particle sizes. Following this approach, we synthesized nanoparticles with sizes between 4 and 7 nm. We investigated their reactivity, and the reactivity of $\text{Ce}_{1-x}\text{Zr}_x\text{O}_2(111)$



Authors (Standing): Xianqin Wang (left) and Jose A. Rodriguez. (Sitting): Jon Hanson (left) and Jan Hrbek

surfaces, towards SO_2 .

Figure 1 shows the structure of an ideal $\text{Ce}_{1-x}\text{Zr}_x\text{O}_2(111)$ surface ($x < 0.4$). The top layer consists of O atoms, but within this layer there are holes that expose the Ce or Zr cations in the second layer.

This well-defined surface allows the detailed study of $\text{O} \leftrightarrow \text{SO}_2$ and $\text{Ce,Zr} \leftrightarrow \text{SO}_2$ interactions. For the $\text{Ce}_{1-x}\text{Zr}_x\text{O}_2$ nanoparticles, the results of transmission electron microscopy show rough surfaces that can be O or cation-terminated and have a high density of edge or corner sites. These different structural properties affect the chemical reactivity of these mixed-metal oxides.

The top of **Figure 2** shows S K-edge XANES spectra for the adsorption of SO_2 on $\text{CeO}_2(111)$ and $\text{Ce}_{0.7}\text{Zr}_{0.3}\text{O}_2(111)$ surfaces at room temperature. A comparison to the corresponding peak positions for sulfates and sulfites indicates that SO_4 is the main species formed on the oxide surfaces, with a minor concentration of SO_3 ($\text{SO}_2(\text{gas}) + n\text{O}_{\text{lattice}} \rightarrow \text{SO}_{3,\text{ads}}$ or $\text{SO}_{4,\text{ads}}$). The cations in the second layer have all of their O neighbors (eight in total), and interact very weakly with an ad-

sorbed SO_2 molecule. One must introduce O_2 vacancies in $\text{CeO}_2(111)$ and $\text{Ce}_{0.7}\text{Zr}_{0.3}\text{O}_2(111)$ to see the interaction of SO_2 with the metal cations and the subsequent dissociation of the molecule.

Figure 2 also shows S K-edge XANES spectra taken after exposing nanoparticles of CeO_2 , $\text{Ce}_{0.66}\text{Zr}_{0.33}\text{O}_2$ and $\text{Ce}_{0.66}\text{Ca}_{0.33}\text{O}_{2-y}$ to SO_2 at 25 °C. Again, we found that SO_4 is the main sulfur-containing species

present on the oxides, but, in addition, we saw features at photon energies between 2470 and 2472 eV that denote the existence of metal-S bonds as a consequence of full SO_2 dissociation. Thus, the nanoparticles have metal cations at corner or edge sites that can interact well with the SO_2 molecule. In addition, there may be O vacancies in the surface of the $\text{Ce}_{0.66}\text{Zr}_{0.33}\text{O}_2$ and $\text{Ce}_{0.66}\text{Ca}_{0.33}\text{O}_{2-y}$ nanoparticles that facilitate S-O bond cleavage.

Figure 3 shows the effect of temperature on the SO_4 signal for the CeO_2 and $\text{Ce}_{1-x}\text{Zr}_x\text{O}_2$ systems in Figure 2. As the temperature is raised, SO_4 decomposes. The SO_4 adsorbed on the nanoparticles is somewhat more stable than that present on the (111) surfaces. For both types of systems, the presence of Zr seems to induce an increase in the thermal stability of the adsorbed sulfate.

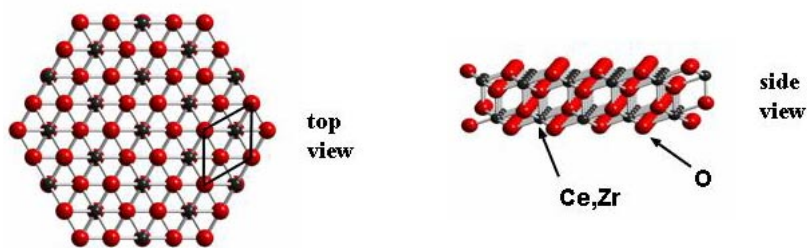


Figure 1. Top and side views of an oxygen-terminated $\text{Ce}_{1-x}\text{Zr}_x\text{O}_2(111)$ surface ($x < 0.4$). The large spheres represent O atoms, and the small spheres correspond to Ce or Zr atoms in a solid solution.

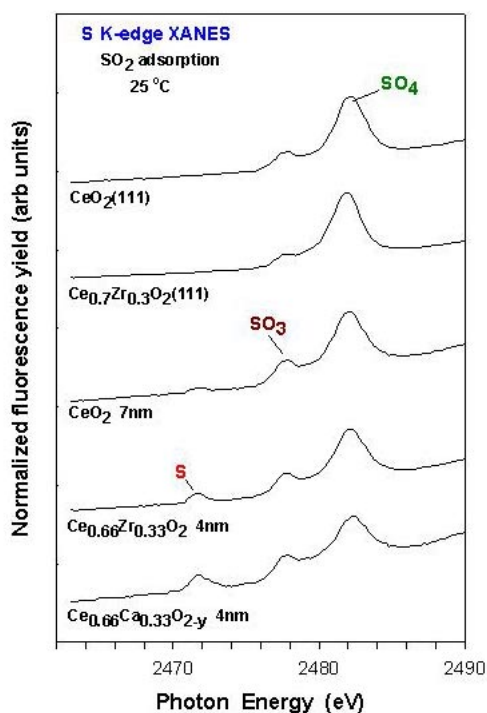


Figure 2. S K-edge spectra taken after dosing SO_2 to $\text{CeO}_2(111)$ and $\text{Ce}_{0.7}\text{Zr}_{0.3}\text{O}_2(111)$ surfaces, and nanoparticles of CeO_2 , $\text{Ce}_{0.66}\text{Zr}_{0.33}\text{O}_2$ and $\text{Ce}_{0.66}\text{Ca}_{0.33}\text{O}_{2-y}$. The samples were exposed to 0.1 Torr of SO_2 for five minutes at 25 °C.

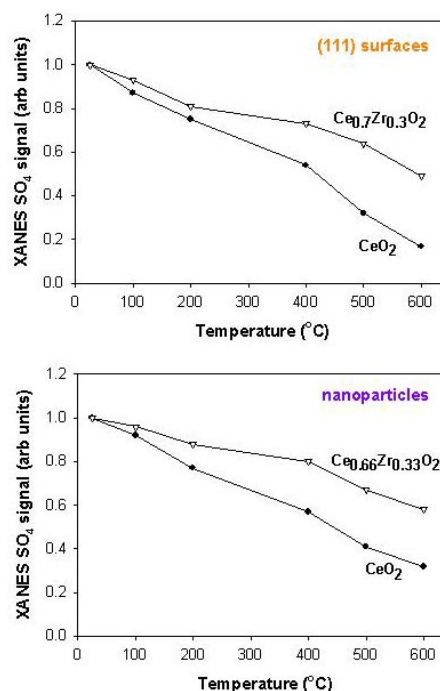


Figure 3. Effect of temperature on the XANES signal for the SO_4 formed on the CeO_2 and $\text{Ce}_{1-x}\text{Zr}_x\text{O}_2$ systems shown in Figure 2. The top panel shows the results for the (111) surfaces, while the bottom panel contains the corresponding results for the nanoparticles.